![Substantia logo]
Substantia
An International Journal of the
History of Chemistry

Data Availability Statement: All relevant data are within the paper and its Supporting Information files.

Competing Interests: The Author(s) declare(s) no conflict of interest.

Feature Article

Boxing Partula: 25 Years After

Stephen T. Hyde

School of Chemistry, The University of Sydney, Sydney, Australia
E-mail: stephen.hyde@sydney.edu.au

Abstract. The comprehension of form generally assumes a euclidean three-dimensional perspective. I argue here that non-euclidean geometry has much to offer in understanding structures of atomic crystals, molecular liquid crystals and related mesoporous inorganic materials and biominerals.

Keywords: Curvature, Crystallisation, Mesostructure, Liquid Crystals, Non-Euclidean Geometry.

I have been pleasantly surprised by the continuing interest of colleagues in the note, which offers an alternative perspective of topologically complex structures from the conventional the-dimensional euclidian view. Hence this slightly updated version. Naturally, my choice of examples to illustrate the thesis that many structure can be fruitfully described as two-dimensional hyperbolic patterns has dated somewhat. For example, the theoretical crystalline schwarzites discussed here remain undiscovered, despite their likely theoretical stability. The focus on such materials has shifted, with more recent report of amorphous schwarzites.

Stephen T. Hyde

1. INTRODUCTION

This essay is a story about "ways of seeing", and how those ways run beneath the more visible tracks that mark the course of the hard sciences. I am interested in exploring the applications of geometry, particularly non-euclidean geometries, to our comprehension of form, shape and dimension. The story is focused on the world of atoms and molecules, and their condensed forms.

The title of this article is adapted from the movies. *"Boxing Helena" is* a provocative film by Jennifer Lynch, that appeared in 1993. Its notoriety centres on the story: an obsessed surgeon keeps a beautiful young Helena – limbless – in a box, in an attempt to capture her heart. Of course, he fails. To this geometer, the movie is an attractive metaphor for the ultimate sterility of conventional euclidean geometric descriptions, that imprison all forms into the box-like grid of euclidean space. Many forms are perhaps better

described within curvilinear grids, which lie at the heart of non-euclidean geometries.

Form is too sterile an issue for most physicists, who opt to explain the energetics of form. Biologists, following Goethe' s example, explore the *morphology* of living things, and classify according to phenotype. I stand betwixt these extremes, asking what are the possibilities of form? and how much are they constrained by the shape of space itself? This is a surprisingly vexed subject, and I can only offer some preliminary insights, which were inspired by the recognition of unusual forms in solid and liquid crystals (explored at length in HYDE *et al.,* 1997; see also VON SCHNERING and NESPER, 1987). However, these insights alone lead to some interesting reflections on the nature of science, and the fragility of some of its unquestioned assumptions about seeing, and perception of shape.

2. MORPHOLOGY IN THE LARGE: SNAIL SHELLS

The writings of the Harvard biologist, Stephen Jay Gould, unfailingly elicit a sense of wonder at the palaeontologists' careful unravelling of the multi-stranded skein of life's evolutionary processes. Gould' s own field is the evolution of land snails. In a recent story, "*Unenchanted Evening*", Gould recounts a poignant tale of the demise of an indigenous Tahitian snail, genus *Partula*, due to the introduction of the voracious *Euglandina* snail by over-zealous and ignorant French scientific bureaucrats (GOULD, 1993). *Euglandina* were introduced in 1977; by 1988, *Partula* was gone forever from most of the islands, and over seventy years of continuous research on *Partula* by a number of eminent snail biologists was abruptly terminated.

This work began in 1917, when Henry Edward Crampton undertook the first of twelve expeditions to the Tahitian islands. Crampton was to spend the next 50 years of his life trekking though the lush, inaccessible terrain of the islands, collecting specimens of *Partula*, followed by painstaking analysis. Crampton compared different populations and the effect of local environment and genetic isolation on the evolution of *Partula*. He elected to index specimens by the shape of their shell. Over 200,000 specimens were subjected to Crampton' s vernier calipers.

The morphology of these shells is pretty much like that of the common garden snail: a twisted and curved cone like the final flourish atop a meringue. To reduce this form to numbers, Crampton made four measurements on each shell, illustrated in the beautiful engraving reproduced in Fig. 1, taken from his own work.
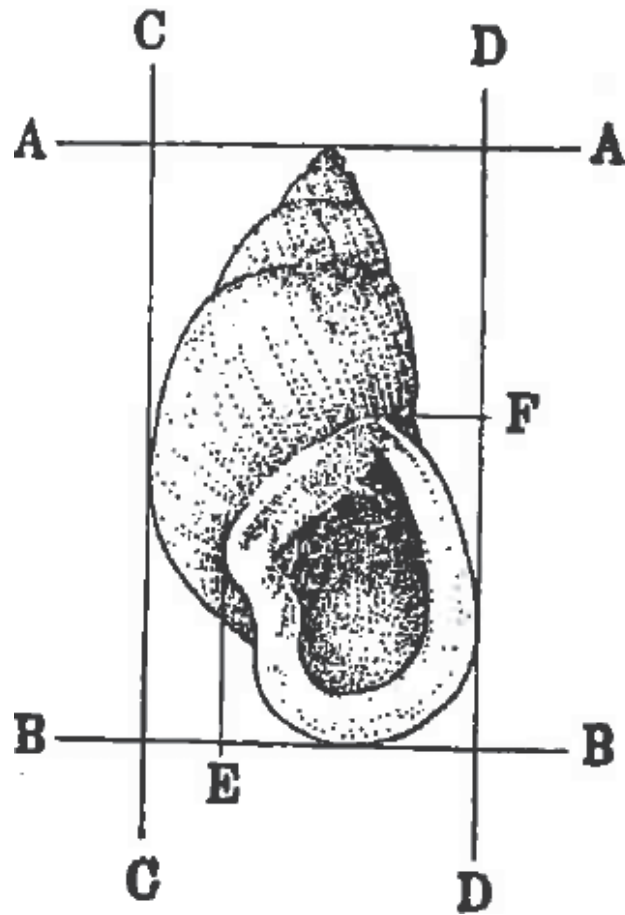

Figure 1. Crampton's engraving of the *Partula* shell, overlayed with his measuring grid.

Notice the rectangular grid imposed on the shell. Crampton measured the lengths AB, FB, CD and ED for each shell, and then calculated averages and standard deviations for each population (to eight significant figures – by hand!).

According to Crampton, "*These figures, together with a single line of text, may be all that represents two to eight weeks of mathematical drudgery … Yet the employment of such methods is justified in the final results.*" (quoted in GOULD, 1993).

How "justified" was the persistent Crampton in his final upbeat assessment of half a century of work? According to Gould, the work ranks with the best evolutionary studies. Yet I can't help feeling that Crampton could have profited better from a more careful choice of metrology of the form of these shells. His rectilinear dimensions seem to me to be a classic case of shoehorning (to borrow a favourite word of Gould), forcing the swirling, twisted shells into flat rectangular boxes: one around the outer form and a second around the opening

of the shell. To recall the analogy with Hollywood: as Helena is constrained by a box, so Crampton' s beloved *Partula* is unnaturally confined between a pair of boxes!

Geometry is a far more versatile tool than the rectilinear lengths Euclid's codification suggest. It underwent a revolution last century, following utter failure to justify Euclid's parallel postulate. After more than two thousand years, the *ad hoc* nature of that postulate was realised, and its removal was shown to yield no collapse of the edifice that is Geometry – rather, a multitude of new "Non-Euclidean" Geometries were immediately erected. Gauss, Lobachevsky, Bolyai, (1820's) and Riemann (1850's) are credited with these advances (although Gauss refused to publicise his findings in the area, terrified of "the clamour of the Boeotians"). The work did not filter through to mathematicians until the end of the last century, largely due to the efforts of Helmholtz in Germany and Clifford in England.

Despite the sea-change in geometry, Euclid's program remains largely unchallenged as the definitive geometry for all but the most curious students of space and form. Rectilinear grids, like Crampton' s, and the euclidean vocabulary of form – polyhedra, spheres and cylinders – are still routinely assumed to span the variety of possible forms in the sciences.

3. MORPHOLOGY OF ATOMS AND MOLECULES

In my own area of research – condensed matter – similar spatial assumptions to that unknowingly invoked by Crampton abound [1]. Consider, for example, the complex atomic arrangements in zeolites. These materials are central to modern society, used as catalysts to "crack" crude oil, forming petrol. Millions of tonnes of a single zeolite catalyst, faujasite, are used annually to make petrol. Zeolites are made up of complex (predominantly) silica frameworks – over one hundred distinct frameworks have been reported to date (MEIER and OLSON, 1992). Although they are solids, the interior of a zeolite crystal is accessible to sufficiently small molecules, which can diffuse along the channels in the framework. From the perspective of non-euclidean geometry (detailed later), they are all surface, and no volume! It is not surprising then that zeolites are excellent catalysts, for catalysts generally work by enhanced reactivity due to surface adsorption (Blum *et al.,* 1993).

Understanding of the chemical functionality of these materials relies on comprehension of their atomic structures: i.e. the relative arrangements of atoms, and bonds, in space. Ball-and-stick models emphasise the topology of the bond network, that links the silica units into an infinite polymer. Alternatively, they are described in terms of packings of convex polyhedra. Examples of both representations are shown in Fig. 2.

Both descriptions are implicitly euclidean and three-dimensional, involving linear links between atoms and plane-faced convex polyhedra. The polyhedral language is a rich one – see for example (O'KEEFFE and HYDE, 1996) – though we shall see it is not necessarily optimal for all purposes.

Our second example of atomic structures concerns allotropes of carbon. The simplest structure of (sp^2 hybridised) carbon is that of graphite, which contains stacked flat hexagonal sheets of carbon atoms. But we now know that this is not the only possible form that sp^2 hybridised carbon polymers can adopt. Warped forms of graphitic carbon result in cage-like fullerenes (Fig. 3).

Fullerenes can be described as faceted balls or rounded polyhedra, in contrast to the extended flat sheets of graphite. The "shapes" of these allotropes can be quantitatively related to their atomic structure by Euler' s equation, which asserts that the numbers of faces *(F),* edges (*E*) and vertices (*V*) in a closed (convex) polyhedron fulfil the condition:

$$V - E + F = 2 \tag{1}$$

We can rewrite this equation in a more useful form for closed polyhedral networks, such as those of the fullerenes. Each ring (a shortest circuit) in the net is a face, and each link between vertices an edge. Denote the number of edges meeting at each vertex by z, and the (average) size of the rings in the network by *n*. For a polyhedral net, containing *R* rings, (1) becomes:

$$\left(\frac{n}{z} - \frac{n}{2} + 1 \right) R = 2 \tag{2}$$

Graphite, whose ring size is equal to 6 and connectivity is equal to 3, can only just be described as a convex polyhedron – an infinitely large one (of infinite radius – flat). Indeed, if $n = 6$ is inserted into (2), the sum

$$\left(\frac{n}{z} - \frac{n}{2} + 1 \right) = \left(\frac{6}{3} - \frac{6}{2} + 1 \right) = 0 \tag{3}$$

so that an unlimited number of rings are required, forming a (flat) infinite polyhedron. On the other hand,

---

[1] With the notable exception of physicists including Maurice Kléman, Jean-Franccois Sadoc, Nicolas Rivier, Remy Mosseri and colleagues, see "Geometry in Condensed Matter Physics", World Scientific, Singapore, 1991.
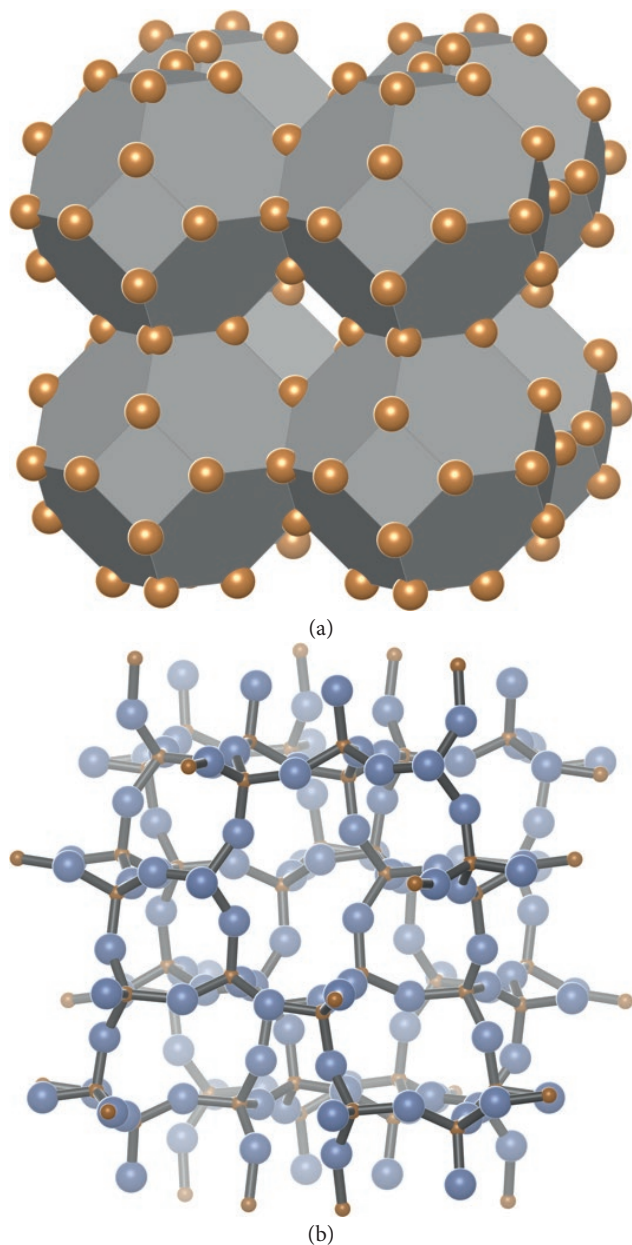
(a)

(b)

Figure 2. Pictures of zeolites: (a) Ball and stick model of the analcime framework. Links represent Si-O-Si bonds in the idealised silicate, balls the Si positions. (b) Polyhedral model of the structure of sodalite (face-sharing truncated octahedra), with Si at the vertices.

if the ring sizes in graphite were exclusively equal to 5, the number of rings, *R,* in a polyhedron fulfils Eq. (2):

$$\left(\frac{5}{3} - \frac{5}{2} + 1\right) R = 2, \quad R = 12 \tag{4}$$

Indeed, the simplest hypothetical closed fullerene contains just twelve 5-rings and twenty carbon atoms
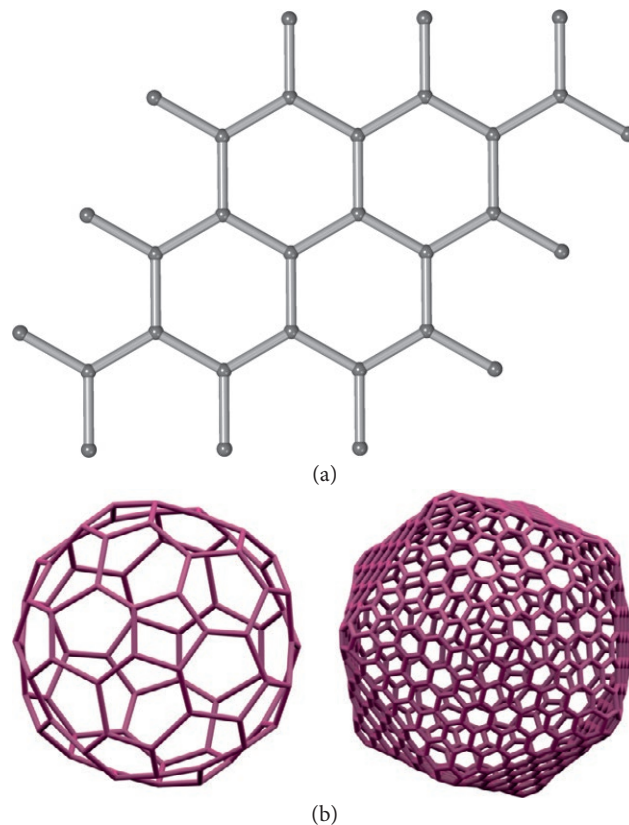

(a)

(b)

Figure 3. (a) The planar network of (three-connected) carbon atoms in graphite, (b) some (three-connected) fullerene networks (carbon atoms lie at each vertex): (L to R) C_{60} and C_{740} (courtesy of Myfanwy Evans).

(C_{20}), lying at the vertices of the Platonic polyhedron, the dodecahedron (Fig. 4).

A curious property emerges from Eq. (2). The addition of an arbitrary number of 6-rings does not change the number of 5-rings in the closed shell polyhedron, since (from (3)), 6-rings do not contribute to the equation. Thus, regardless of the number of 6-rings, twelve pentagons – and only twelve – are to be found in all closed-shell fullerenes (built of 5- and 6-rings). If more than 12 pentagons are inserted, Eq. (1) no longer holds, and the network instead continues to spiral inwards around itself, producing a network which shares many of the characteristics of the *Partula* shell. The network no longer closes on itself seamlessly, but contains spiral edges, shown in Fig. 5. Such exposed edges – along which the carbon atoms have only two bonds – are not going to remain so for long. These structures are unlikely to form under normal conditions.

What happens if 7- or 8-rings are introduced to these three-connected networks? From Eq. (2), it is clear that the presence of these rings precludes the formation of convex or flat polyhedra, since
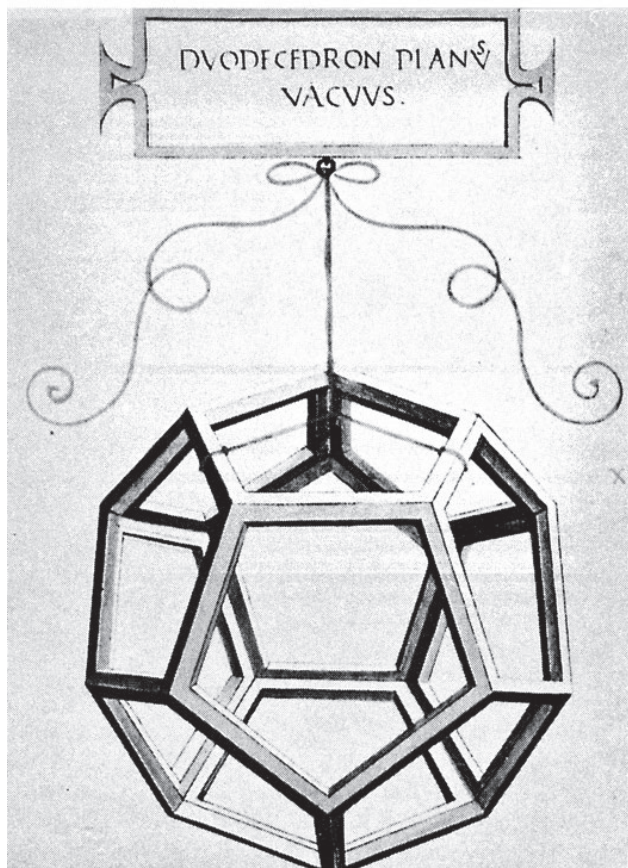
Figure 5. Kroto and Mackay's hypothetical spiral graphitic carbon structures, adapted from KROTO (1988).

Fig. 4. Da Vinci's engraving of a regular dodecahedron, whose vertices locate the relative positions of carbon atoms in the fullerene, C20.

$$\left(\frac{n}{z} - \frac{n}{2} + 1\right) = \frac{2z + (2-z)n}{2z} = 1 - \frac{n}{6} \tag{5}$$

is negative (so that formally, a negative number of rings must be found in the convex polyhedron, cf. Eq. (2)). To cope with the shapes formed by three-connected networks containing larger rings than 6-rings, we need to generalise Euler's equation (1), introducing a new parameter, χ, known as the Euler-Poincare characteristic.

$$\left(\frac{n}{z} - \frac{n}{2} + 1\right) = \chi \tag{6}$$

The contribution to the Euler-Poincare characteristic of 7- and larger rings is, from Eq. (5) above, negative. What does this mean in space?

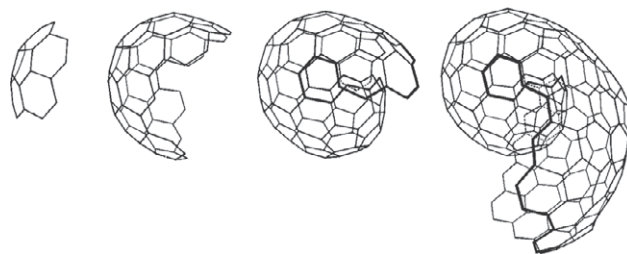Three-connected nets containing >6-rings are forced to warp, so that they lie on saddle-shaped surfaces, in contrast to the convex polyhedral surfaces formed by 5-rings. It is useful to think of the curving of graphite layers as a disclination process: 5- and 7-rings resulting in positive and negative disclinations respectively (Fig. 6).

The saddle-shape that results by insertion of negative disclinations in graphite is most evident when the average ring-size is close to 6, but slightly larger. (This situation can be realised simply by inserting a large number of hexagons into a cluster of 7-, 8-, … rings, since the hexagons do not affect the value of the characteristic, χ) Depending on the number and arrangement of heptagons or octagons, seamless crystalline porous frameworks or disordered sponge-like sheets can result, analogous to the boundary-free fullerenes shown in Fig. 3.

The Euler-Poincare characteristic, (Eq. (6)), is "quantised" for boundary-free surfaces, and related to the number of channels within surface. If the underlying surface is periodic, the characteristic per unit cell is likewise quantised, and so discrete families of frameworks containing 7-, 8-, … rings are possible, analogous to the twelve 5-rings present in a closed shell fullerenes containing only 5- and 6-rings. Such structures have been proposed as possible modifications of graphitic carbon. They have been christened "Schwarzites", in honour of the celebrated nineteenth-century German mathematician, Hermann Amandus Schwarz (MACKAY and TERRONES, 1991). Examples of hypothetical schwarzite frameworks are illustrated in Fig. 7.

What happens as the density of negative disclinations (and the average ring-size) increases? For example, insertion of 8-rings, rather than 7-rings results in frameworks that are no longer clearly sheet-like, rather they appear three-dimensional, and morphologically similar to zeolite frameworks (Fig. 8).

Geometrically, no quantitative transition accompanies this apparent shift of form of three-connected schwarzite frameworks with increasing disclination density; rather our perception of the structural form is changing. When the ring-size barely exceeds six, the larger rings surrounding tunnels of the network are perceived to be open, while we mentally "fill in" the
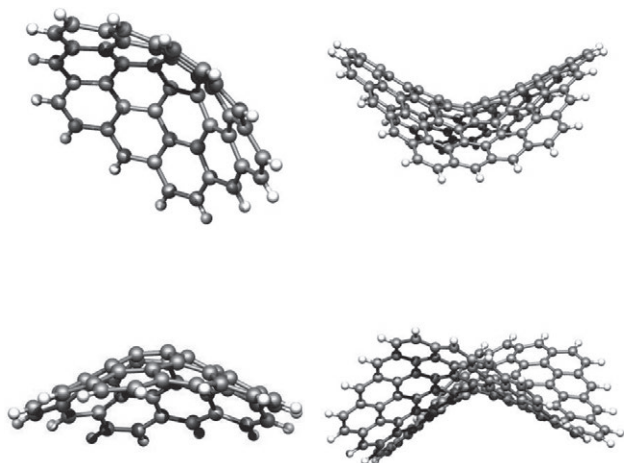
Figure 6. (Left/Right) The formation of rings less than/greater than 6-rings in a flat graphite sheet (tiled by hexagons) leads to positive/ negative disclinations. Copyright Chris Ewels (www.ewels.info).
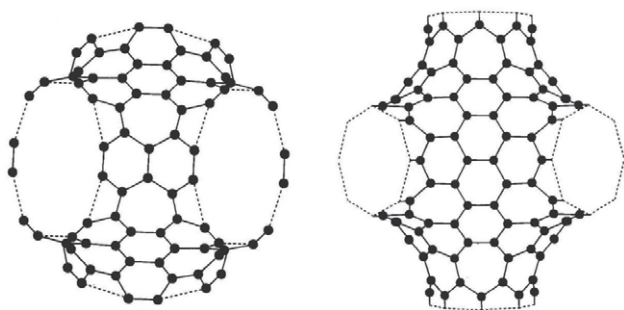

Figure 7. Bonding networks in some hypothetical crystalline "schwarzites", due to LENOSKY *et al.* (1992) (confined within a unit cell). The average ring-sizes here are equal to 6.2, including 6- and 7-rings only.

smaller rings, to form a continuous (and open) saddle-shaped sheet. By contrast, when the ring-size in the surface becomes significantly larger than six, the rings surrounding pores approach the same size as the rings in the saddle-shaped sheet, and we mentally fill in tunnels (closing them off) and sheet-rings, leading to the (closed cell) infinite-polyhedral description, such as the sodalite description shown in Fig. 2. An apparently uniform network twists through space, and the structures are perceived as conventional three-dimensional frameworks.

Complex zeolite-like morphologies can also be found in molecular materials. It now appear that porous arrays are common in macromolecular assemblies, including biological systems (GUNNING, 1965; LANDH, 1995; HYDE *et al.,* 1997). These shapes too lie beyond the usual vocabulary of (euclidean) form, and
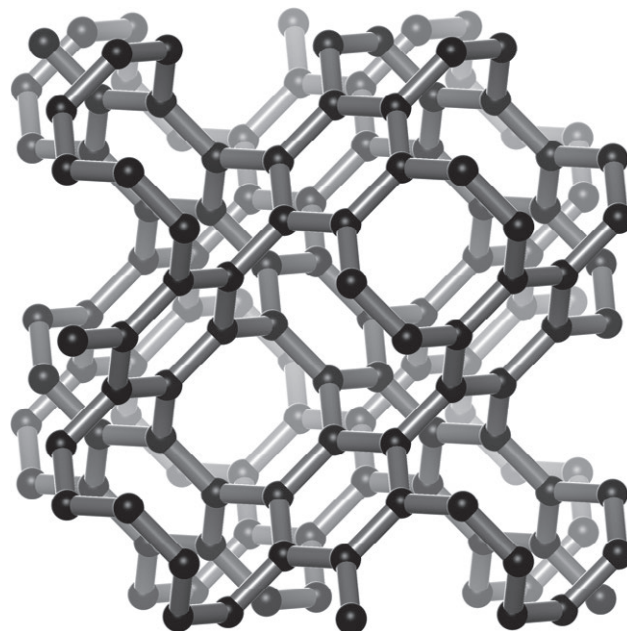
(a)
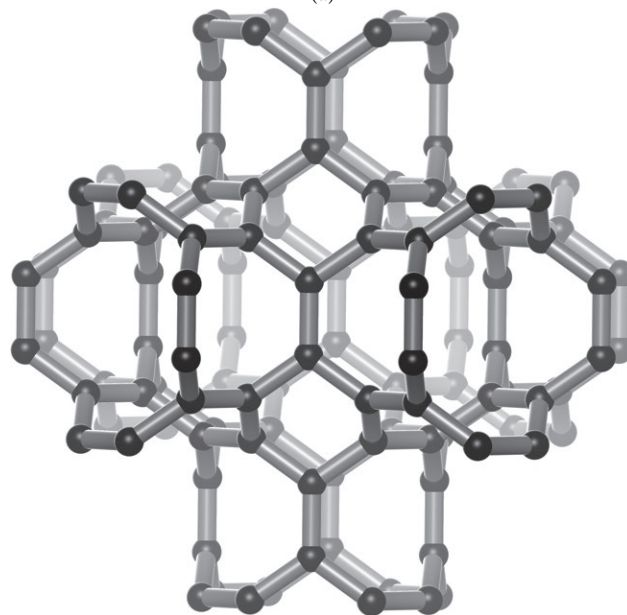
(b)

Figure 8. Cubic schwarzites containing only 6- and 8-rings: poly-benzene (a) *D* and (b) P (O'KEEFFE *et al.,* 1992).

descriptions have inevitably been deficient. For example, biologists studying the shapes of organelles within cells have resorted to exotic terms such as "undulating tubular bodies" or "tubulo-reticular structures" to account for the complex forms deduced from stained optical-microscopic sections of membranes in cells (Fig. 9).

Whereas the channels in zeolites are typically a few Angstroms in diameter, those in cell organelles are
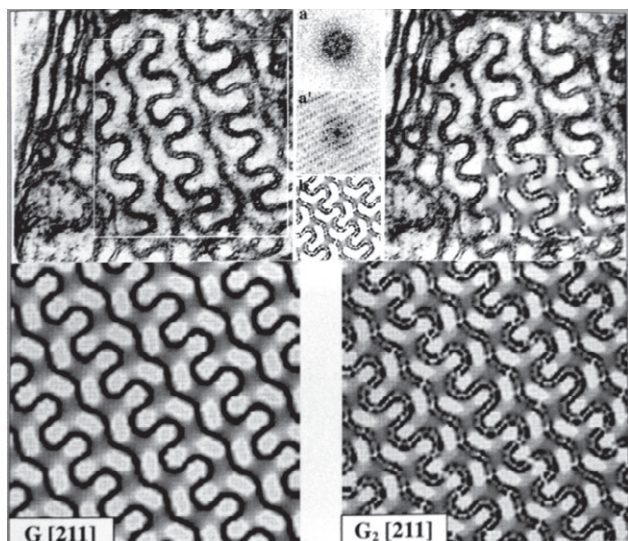
Figure 9. Stained sections through the pro-lamellar body (the light-harvesting photosynthetic centre) of a dark-adapted plant. (Insets: Fits due to Landh, described later in the text.) Adapted from HYDE *et al.* (1997).

Figure 10. LUZZATI and SPEGT'S model (1967) of the mesostructure of a cubic phase, consisting of two intertwined rod networks, enclosing water (reversed phases) or the lipid/surfactant chains (normal phases).

Figure 11. Electron micrograph of silica templated from a copolymer material, whose nanostructure (inset) corresponds to a single rod network in Fig. 10. Image courtesy of Hirokazu Hasegawa.

microns. The very large dimensions of cell membranes are not yet understood.

The major component of cells is the lipid bilayer. Synthetic bilayer membranes can be reconstituted *in vitro* using only lipids (and water). Lipids, or related synthetic surfactant molecules (collectively called surfactants), spontaneously assemble in water to separate the oily chains – which abhor water – from the polar and water-soluble head groups. In some cases, namely "bicontinuous cubic phases" of surfactant- or lipid-water mixtures, the membranes display identical morphologies to those of the organelle membranes. These structures were originally described in terms of intertwined arrays of channels (Fig. 10), similar to the tunnel arrangements in zeolites (LUZZATI and SPEGT, 1967). In contrast to the membranes *in vivo,* the channels of these *in vitro* membranes are typically 20-50 Å across.

Identical structures are also found in inorganic materials "templated" with surfactants, with pore sizes ranging between 20-150 A (BECK *et al.,* 1992; ALFREDSSON and ANDERSON, 1996), and copolymer mixtures (typically 1000 A diameter) (HASEGAWA *et al.,* 1987, 1993; HAJDUK *et al.,* 1994) (Fig. 11).

It turns out that there are deep structural similarities between zeolites, schwarzites, surfactants and polymer molecular aggregates. In fact, all of these materials can be described by a generic structural *motif,* the hyperbolic surface. These materials can be related to periodic hyperbolic surfaces. The most prevalent examples found to date
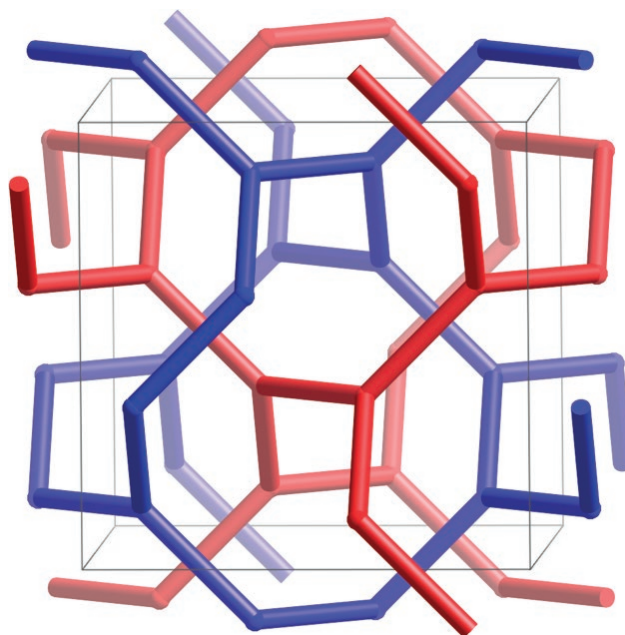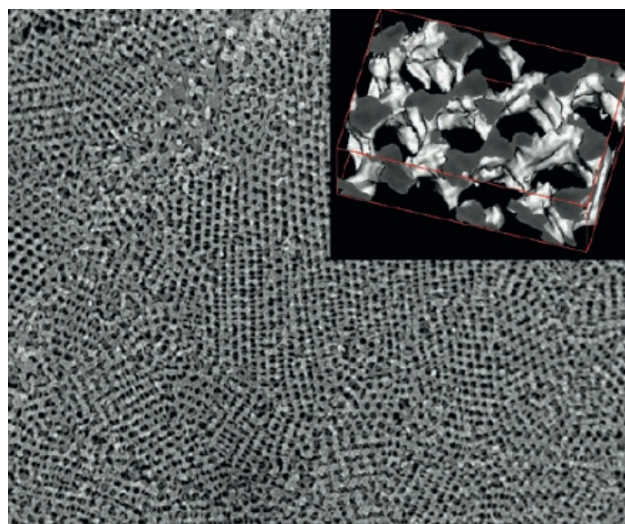
are cubic surfaces: the D-surface (or "diamond" surface), the *P* surface and the gyroid, shown in Fig. 12.

The possibility of describing "three-dimensional" atomic frameworks, such as those of zeolites and schwarzites, in terms of two-dimensional hyperbolic spaces is
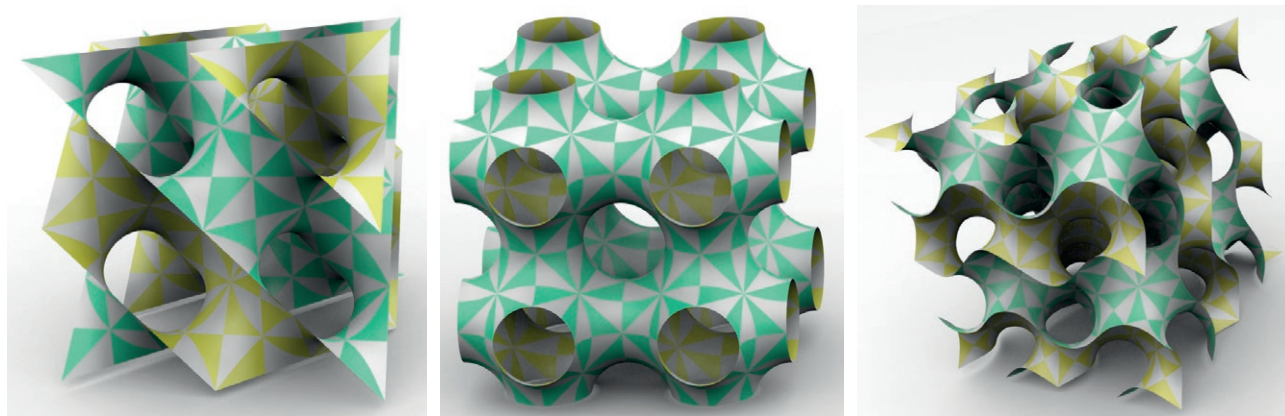
Figure 12. (Left to right) Portions of the D-surface, the *P* surface and the gyroid. Figure courtesy Myfanwy Evans.

evident in the examples shown in Fig. 13. Some molecular assemblies too are perfectly described in terms of these surfaces. For example, the membrane sections agree exactly with calculated sections through the *D* surface (insets, Fig. 9). In order to map these frameworks onto two-dimensional hyperbolic space, the edges of the frameworks must be curved, to form geodesics in that space.

Description is the first stage of science. I hope that the examples shown above reveal the complexity of this step alone, and the dangers inherent in too limited a catalogue of form. The next step requires some explanation of why that description is a useful one. Some progress has been made towards that second goal, outlined below.

4. DIFFERENTIAL GEOMETRY, NON-EUCLIDEAN GEOMETRY AND TOPOLOGY

In order to appreciate the nature of non-euclidean structures, the concept of dimensionality and the importance of periodic hyperbolic surfaces in these materials, we need first to digress a little into geometry.

No-one is able to offer a complete catalogue of form. Geometric studies following the program outlined by Riemann in 1853, and still in progress, suggest that the variety of forms relevant to physical systems in n-dimensions (n-manifolds) is rich. The problem of enumerating all four- (and higher dimensional) manifolds is unsolvable; the jury is still deliberating in the case of three-manifold (THURSTON, 1997). Two-dimensional surfaces can however be catalogued to a limited degree using concepts from differential *geometry* and *topology*. Differential geometry is concerned with the local shape of a surface – the shape of a small patch on the surface. By contrast, topology deals with the global structure, the connectivity, of the surface.

The shape of a surface patch can be succinctly described by its Gaussian curvature, which can be positive, negative, or zero (Fig. 14).

Surfaces of zero Gaussian curvature are called flat, despite the fact that they can be planar, cylindrical or conical. Why? Because it turns out that a rectangular flat grid, such as that adopted by Crampton, can be wrapped onto any surface of zero Gaussian curvature, without distortions of the distances between vertices or the right-angles between edges (measured along the surface patch rather than through space). This fact is known to us all: a flat sheet of paper can be wrapped onto a cylinder without any stretching or crinkling.

The case of zero Gaussian curvature is that examined in detail in euclidean geometry. The other cases correspond to (two-dimensional) non-euclidean geometries: saddle shapes belong to *hyperbolic* geometry and spherical (or ellipsoidal) caps to *elliptic* geometry.

In fact, Euclid also analysed other shapes, such as polyhedra, and spheres. But he saw these shapes exclusively within the context of three-dimensional (flat) space – in his view the convex polyhedra and sphere marked the boundaries of a filled inner volume. Within the curved two-dimensions lying on the surface of these forms, many geometrical features would have surprised Euclid. For example, a triangle – all of whose sides are "lines" in the sense that they are the shortest trajectories between the vertices (great circles) – can be traced on the sphere whose vertex angles sum to $3\pi/2$, rather than the customary π (Fig. 15).

A sheet of paper *cannot* be wrapped onto a sphere without folding the paper so that some doubling up occurs. In the process, the euclidean rectangular grid drawn on the sheet becomes distorted, and lengths and/or angles within the grid on the sphere are no longer the same as those in the original flat grid. Indeed, the
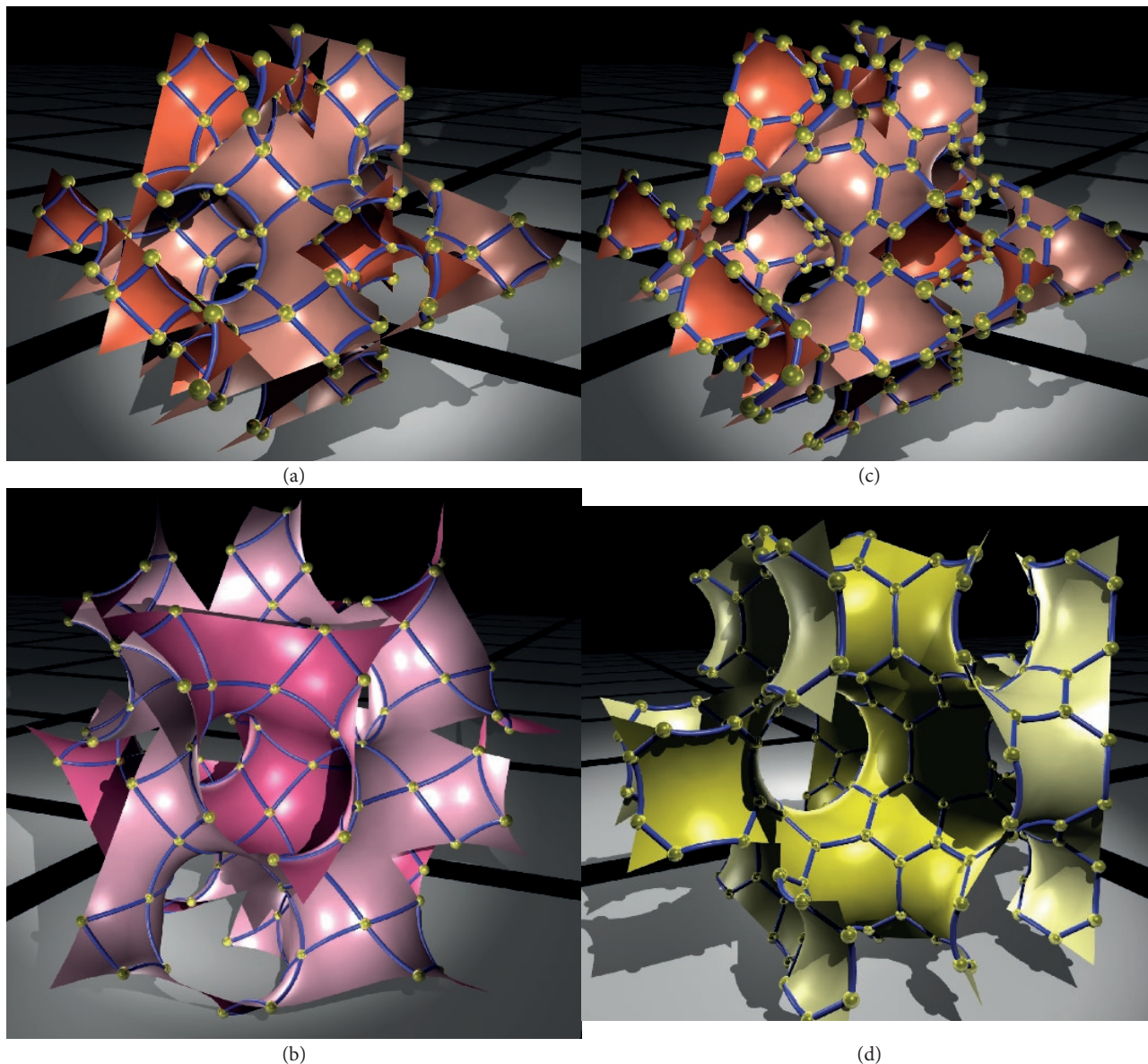
(a)

(c)

(b)

(d)

Figure 13. (a): The sodalite zeolite framework lying in the D-surface. Vertices of the framework occupy identical cartesian locations to those in Fig. 2, the edges have been curved to lie in the surface. (b): Fragment of the analcime framework in the *D* surface, marked in black on the surface. (c), (d): Two schwarzite frameworks: polybenzene *D* and *P*. (Pictures courtesy of Stuart Ramsden.)

elliptic cap – of positive Gaussian curvature – results from excision of a sector from the plane and reglue-ing. Similarly, if a wedge is inserted into the flat sheet, a hyperbolic saddle-shape results, of negative Gaussian curvature.

This local classification scheme based on Gaussian curvature may appear at first sight trivial, but it is the simplest universal geometric classification. Look, for example, at the shapes of potato crisps (Fig. 16): you'll find blistered chips, of positive Gaussian curvature, flat portions (zero Gaussian curvature) and saddles (negative Gaussian curvature)!

Another happy hunting ground for local shape can be found in leaves. (This was first pointed out to us by William Thurston.) Cabbage leaves, for example, are elliptic, many eucalyptus leaves are euclidean, and mignonette (or "coral") lettuce leaves are decidedly hyperbolic. Some examples are shown in Fig. 17.

The rich structural variety within the hyperbolic domain – readily apparent from the variety of shapes
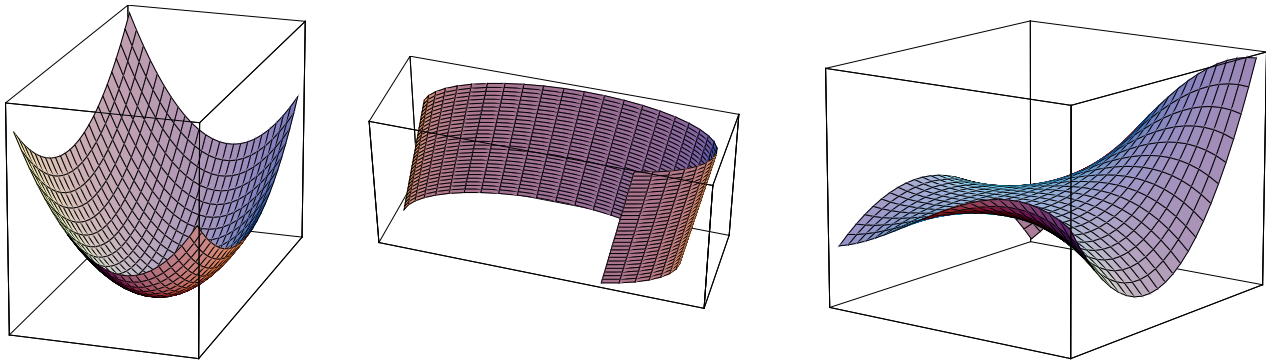
Figure 14. Caps, sheets and saddles with positive, zero, and negative Gaussian curvature.
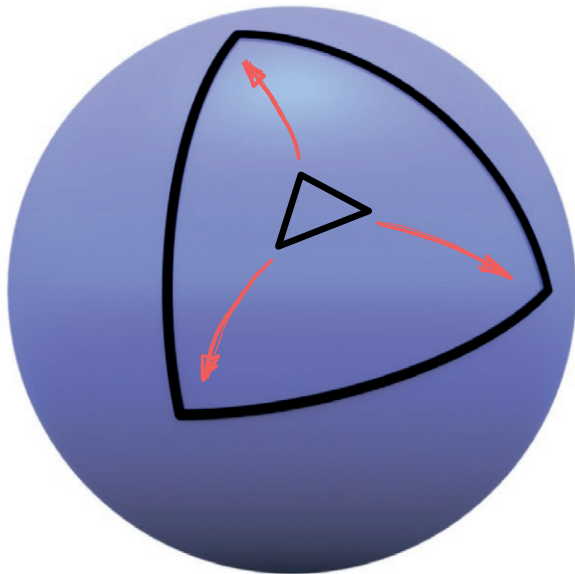

Figure 15. A flat euclidean triangle placed on the sphere builds a spherical triangle, whose vertex angles add up to an angle exceeding to 180°: the example shown has an angle sum of 270°. Figure courtesy Myfanwy Evans.

Figure 16. The variety of surface form in potato crisps.

in mignonette leaves – is difficult to appreciate without some familiarity with the concepts of global structure, described in part by the topology of the surface. Topology is often called "rubber sheet geometry", since surfaces which can be bent into each other (without tearing or gluing) are topologically equivalent.

For example, all convex polyhedra are topologically equivalent (called "homeomorphic") to the sphere. Imagine a rubber balloon stretched over an inner skeleton shaped to form the edges of a polyhedron. Blow the balloon up more, until the skeleton rattles within it – a sphere results. Topologically speaking, convex polyhedra and spheres are indistinguishable – all have an Euler-

Poincare characteristic of two (Eq. (6)). The difference between spheres and faceted convex polyhedra lies in their distribution of Gaussian curvature over the surfaces; for the sphere it is everywhere homogeneous, while it is concentrated at the isolated vertices of polyhedra.

For two-dimensional surfaces in three-dimensional euclidean space, geometry and topology are inextricably linked by the Gauss-Bonnet theorem. This theorem reveals the importance of Gaussian curvature in a topological sense. To understand the theorem, we need to introduce a dimensionless curvature measure: the "integral curvature", which is defined to be the integral of the Gaussian curvature ($\iint_{surface} K da$) over the area of the surface.

This integral curvature is proportional to the Euler-Poincare index, provided the surface is closed, and thus free of boundary arcs:

$$\iint_{surface} K da = 2\pi\chi \qquad (7)$$

This result is strikingly succinct. It asserts that no matter how a surface is stretched or squashed, its integral curvature remains fixed, since these distortions do not affect the Euler-Poincare index. In other words, its

Figure 17. (L to R): Cabbage (elliptic), eucalyptus (parabolic) and lettuce (hyperbolic) leaves with positive, zero and negative curvature.

Gaussian curvature distribution and area are coupled to give constant integral curvature. The Euler-Poincare index is simply related to another topological measure, known as the "genus" of the surface. For the usual "two-sided" surfaces the surface genus, *g,* is related to the Euler-Poincare characteristic by the equation:

$$\chi = 2 - 2g \qquad (8)$$

(The formula does not hold for "one-sided" or "non-orientable" surfaces, such as the Mobius strip, or for surfaces with boundary arcs.)

The shape – give or take the bending or stretching allowed within topology – of *any* orientable surface is always homeomorphic to a single sphere, decorated with some number of distinct handles. An orientable surface of genus *g* is topologically equivalent to a sphere with *g* handles, so that the genus is equal to the number of handles. That is the origin of the quantisation of topology mentioned above. Thus the *average* value of the Gaussian curvature, $\langle K \rangle$, defined by the ratio of the integral curvature to the surface area,

$$\langle K \rangle \equiv \iint_{surface} K \, da / \iint_{surface} da$$

is positive for genus zero surfaces, zero for genus one, and negative for genus two, three, … surfaces. This topological characterisation offers a useful classification of surface forms.

Convex polyhedra, which are homeomorphic to the sphere, are genus zero forms. The next case, genus one, includes all donut-shaped surfaces, cups, … all are homeomorphic to a sphere with one handle (illustrated in Fig. 18).

Since the donut has a genus equal to one, its average value of the Gaussian curvature vanishes, and its average geometry is flat! How is this so? Well, the integral curvatures of the hyperbolic and elliptic regions cancel exactly, no matter how asymmetric the torus: from a coffee cup, or a ball with a single tiny handle spanning its surface (Fig. 19). We say that the donut is *inhomogeneous,* in that its Gaussian curvature changes from point to point along the surface.

The "flat torus" is a donut-shaped surface – unrealisable in euclidean three-space, but realisable in three-dimensional spherical space – which is *homogeneous* in its Gaussian curvature. Thus, its Gaussian curvature is everywhere zero, in contrast to the inhomogeneous donut in three-dimensional euclidean space, whose Gaussian curvature oscillates about zero. The flat torus can be reticulated with a distortion-free square (two-dimensional Cartesian) grid of arbitrary mesh size.

A particularly interesting way to represent the torus, which reveals its average euclidean geometry follows from gluing of opposite edges of a rhombus. If the horizontal edges of the rhombus are glued together, a cylinder results. Gluing the other pair of edges (now loops), closes the cylinder on itself, forming a torus (Fig. 20).

Given our interest in spatially periodic structures, which underlie the arrangement of atoms in crystals, this is a very suggestive construction, reminiscent of the repeated zone scheme in quantum mechanics, and Born-von Karmann boundary conditions. Indeed, this construction allows a single unit cell of the two-dimensional

Figure 18. Homeomorphism between a donut, a sphere with one handle and a cup. Image from Roy and Kesselman, ArXiV 2201.06923.
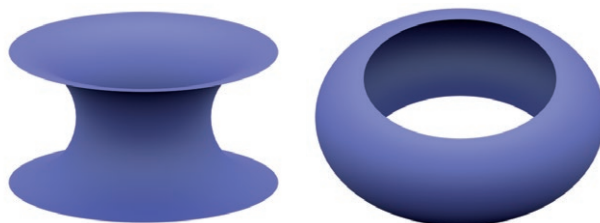

Figure 19. Decomposition of a torus into (left) a hyperbolic surface (K<0) and (right) an elliptic surface (K>0). On average, the torus is flat, as the hyperbolic and elliptic fractions have equal and opposite integral curvatures, for any torus, regardless of its particular geometry.

Figure 20. Gluing protocol for a torus from a rhombus. Figure courtesy Myfanwy Evans.

lattice, or periodic array (the rhombus), to be mapped into the torus.

An infinite two-dimensional lattice can be wrapped an infinite number of times around the torus, covering the torus once for each unit cell. (In mathematical jargon, the plane, tiled by a two-periodic lattice, is the *universal cover* of the torus.)

The construction begs to be extended to the domain of true crystals which exhibit three-dimensional lattices. In this case, the unit cell is a rhombohedron. Just as (opposed) *edges* separated by a lattice vector of the two-dimensional lattice are glued to form the torus, opposite *faces* of the unit cell can be glued to form a three-dimensional (solid) version of the torus, called naturally enough, the 3-torus.

Alternatively, we have seen that three-periodic hyperbolic surfaces can be used to describe three-periodic structures, by mapping these three-dimensional structures onto the two-dimensional crystalline hyperbolic surfaces. These infinite surfaces have unbounded genus. However, they have a finite number of handles within a single unit cell, and they can be catalogued according to their symmetries, and genera per unit cell. The unit cell topology is that of the boundary-free surface, formed by imposition of Born-van Karman boundary conditions, "gluing" boundary elements in pairs. Since they contain three independent lattice vectors, they must have genus (at least) three per unit cell, in contrast to the (genus-one) torus characterising a two-dimensional planar lattice. If the "unfolding" procedure of Fig. 20 is generalised to a higher genus g-torus, the resulting "flattened" surface is a polygon containing (at least) 4g sides (just as the torus of genus

one gives a four-sided rhombus), shown in Fig. 21 for a two-torus.

It was noted above that the flat torus – a homogeneous parabolic structure (i.e. of constant Gaussian curvature) – is unrealisable in euclidean three-space. Are there homogeneous hyperbolic surfaces in this space? This question is a deep one, which was answered partially in a famous paper on non-euclidean hyperbolic geometry by the Italian geometer Beltrami in 1856 (STILLWELL, 1982). Just as euclidean (two-dimensional) geometry lies in the flat plane, hyperbolic geometry lies in the so-called "hyperbolic plane". Beltrami showed that some essential features of the hyperbolic plane were to be found in a homogeneous hyperbolic surface, called the "pseudosphere", shown in Fig. 22. In fact, the hyperbolic plane can be considered as the universal cover of the pseudosphere, since it wraps an unlimited number of times about the pseudosphere (STILLWELL, 1982).

Notice that this surface contains a cusp at its waist. Early this century, David Hilbert proved that any homogeneous hyperbolic surface in euclidean three-space necessarily contains such singularities. In the terminology of contemporary condensed matter physics, hyperbolic geometry is necessarily "frustrated"[2] in our space, unlike (two-dimensional) euclidean or elliptic geometries.

"Pseudosphere" refers nowadays to any surface of constant negative Gaussian curvature. All such surfaces

---

[2] An uncharacteristically emotive term for physicists, perhaps misplaced. After all, the frustration lies with us rather than condensed matter!
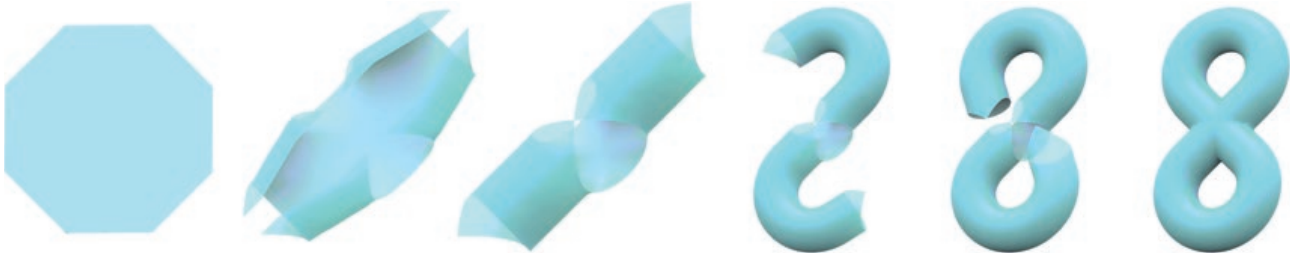
Figure 21. An octagon can be glued to form a genus two surface. Figure courtesy Myfanwy Evans.
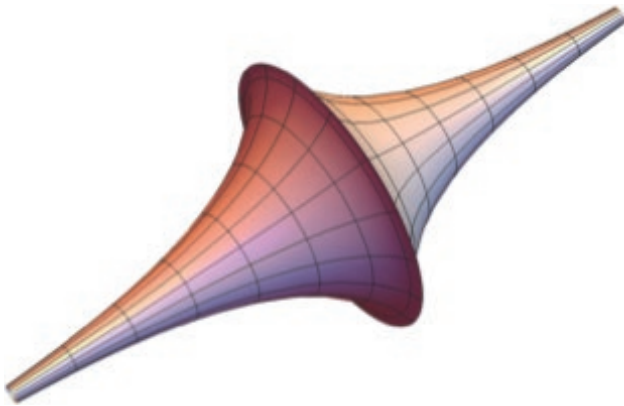

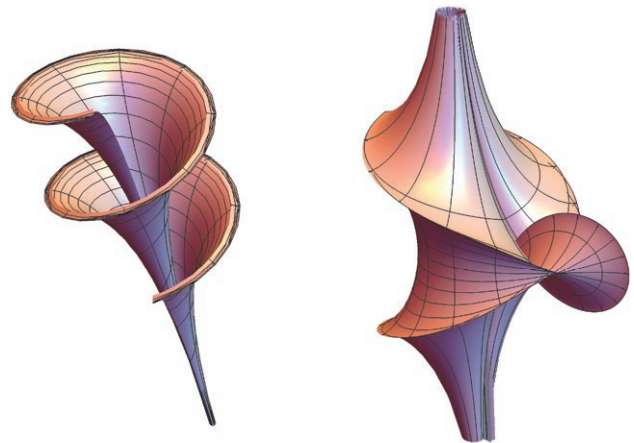**Figure 22.** The pseudosphere, a surface of constant negative Gaussian curvature.

Figure 23. Some pseudospheres: (Left) A cusp-free section of one member of Dini' s surfaces. (Right) Kuen's surface, including cusps.

are equivalent in a two-dimensional sense, despite the fact that their global shapes – their embedding in euclidean three-space – can vary. Other examples are shown in Fig. 23.

A simple model of the pseudosphere can be constructed from the euclidean plane as follows. Build a plane from equilateral triangles – six around each vertex, in order to tile the plane without overlap or gaps. Now insert a seventh triangle at each vertex (a negative disclination), and stitch the "plane" back together. As the size of the plane grows, the structure becomes less and less rigid, and a number of different global shapes can be formed. The presence of tunnels – common to the more complex hyperbolic surfaces – can be seen in the natural tendency of the sheet to wrap onto itself, surrounding open "pores". Indeed, as the warped plane grows outwards, the surface is forced to either self-intersect or spiral around itself (Fig. 24). This feature of hyperbolic geometry can be ascribed to the limited "space" available to contain surfaces in three-dimensional euclidean space: there is not enough room to contain the hyperbolic plane.

Many leaves, particularly ivies, display locally homogeneous two-dimensional hyperbolic geometry.

Adjacent portions of growing leaves necessarily crowd onto each other, and further growth cannot continue without deforming their homogeneous form, and flattening the growth fronts (Fig. 25). The inhomogeneous geometry of these leaves is due to the structure of three-dimensional euclidean space itself!

This frustration – inherent to homogeneous hyperbolic geometry – means that we need to look beyond pseudospheres and consider nearly-homogeneous hyperbolic surfaces, free of cusps. The best candidates found to date are the three-periodic hyperbolic surfaces. (The simplest examples of these surfaces are called Infinite Periodic Minimal Surfaces, or IPMS, named by Alan Schoen, the NASA physicist who discovered many examples in the 1960's (SCHOEN, 1970).)

While these surfaces are free of cusps, their Gaussian curvature varies from point to point, and they are inhomogeneous. Further classifications of IPMS can be made. We consider here only those (orientable) surfaces which are free of self-inter sections (also called embedded triply periodic minimal surfaces, of ETPMS). Examples of IPMS (which are all embedded) are shown in Figs. 12 and 26.
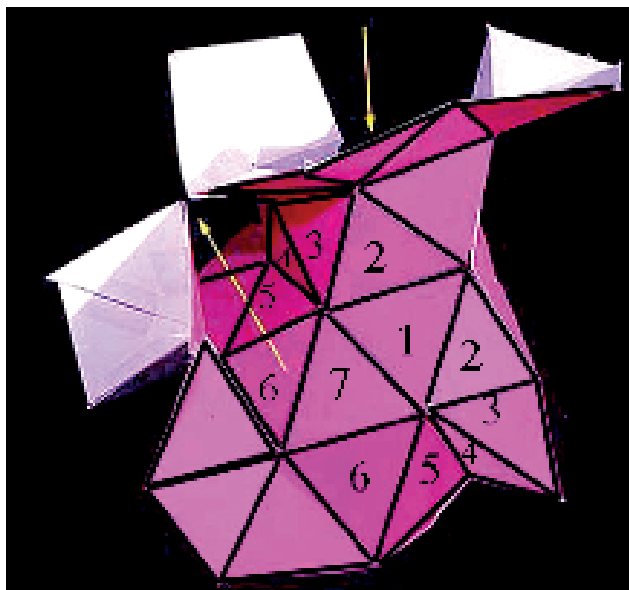
Figure 24. A faceted model of the hyperbolic plane, containing seven equilateral triangles at every vertex. The arrows mark pores.

The importance of IPMS lies principally in their topological structure, rather than their local geometric form characteristic of minimal surfaces (zero average curvature). They provide us with a much fuller catalogue of surface form than had been available until very recently. In many physical systems, the structures formed need not be precisely minimal surfaces (i.e. equally concave and convex at all points on the surface).

It appears that the most nearly homogeneous hyperbolic three-periodic minimal surfaces are those of genus three per (geometric) unit cell and cubic crystallographic symmetry: the *D, P* and gyroid surfaces illustrated in Fig. 12. These crystalline surfaces are topologically the most complex hyperbolic forms possible (of unbounded genus), and it may seem surprising that they are nearly homogeneous structures in our space. But lower genus hyperbolic forms necessarily contain elliptic regions, or boundary "ends" that are asymptotically flat; both cases lead to larger curvature inhomogeneities than those of IPMS and related surfaces. It is more difficult to compare the homogeneity of crystalline hyperbolic surface with related "molten" surfaces. But limited data reveal that the homogeneity of minimal surfaces increases with genus per unit cell, so that crystalline surfaces are naturally favoured. Some examples of genus three and four surfaces are illustrated in Fig. 26.

If that hypothesis is confirmed, it offers a novel view of crystallinity in the physical world. The conventional three-dimensional euclidean perspectives ascribes crys-

tallinity to long-range interaction across space (and minimisation of the resulting energies). Within a hyperbolic perspective however, the induction of three-dimensional periodicity may be driven by the local (and two-dimensional) requirement of minimisation of curvature variations. The occurrence of triply-periodic hyperbolic forms is the natural consequence of a striving for a single preferred curvature. The physical meaning of curvature – a hitherto "hidden variable" – can be recast into more conventional terms, described below.

5. QUASI-HOMOGENEOUS HYPERBOLIC FORMS IN CONDENSED MATTER

Euler's equation, and its generalisations, imply that the generic form of a network depends only on the average ring size and network connectivity. From Eq. (7), a
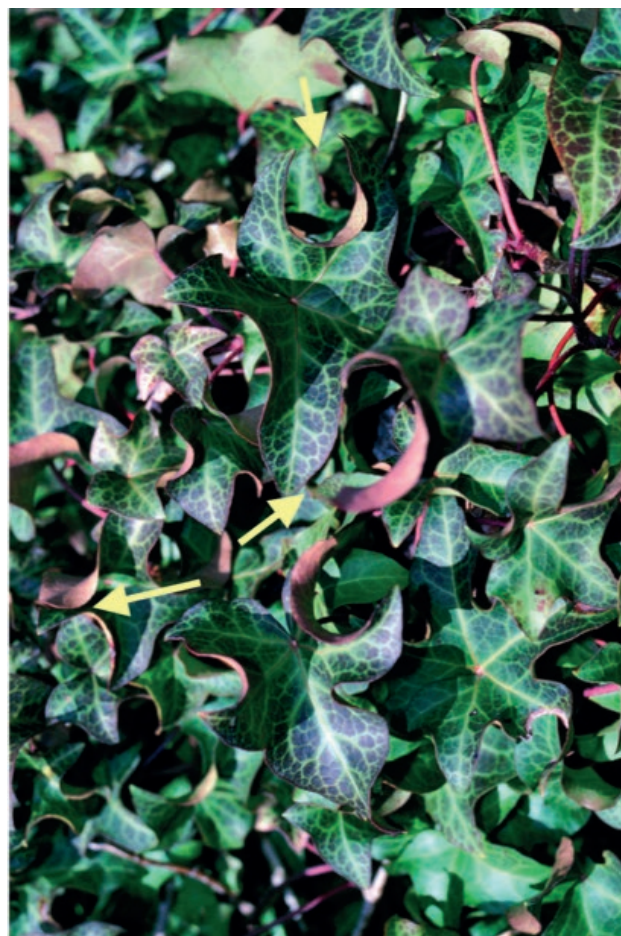

Figure 25. Some nearly-homogeneous hyperbolic leaves (arrowed) in an ivy. Notice the crowding of growing leaves, particularly evident in the arrowed leaves.
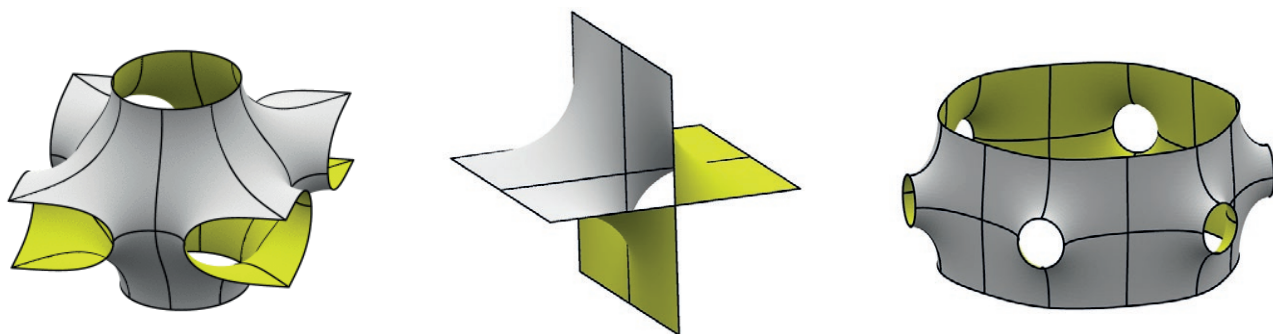
Figure 26. Unit cells of some IPMS (left to right): S'-S" surface (genus 4), CLP surface, H'-T surface (both genus 3). Images courtesy of Ken Brakke.

Figure 27. The shape of a bread-slice can be changed by selective grilling. If the flat slice (left) is grilled on one side only, it becomes elliptic (middle); further grilling of the other side as well gives a hyperbolic slice (right).

hyperbolic layer structure results whenever the Euler-Poincare characteristic is negative, once the average ring size in the network, n, and the connectivity of the network, z, fulfills the inequality (cf. Eq. (6)):

$$\left(\frac{n}{z} + \frac{n}{2} + 1\right) < 0 \; i.e. \, (n-2)(z-2) > 4 \qquad (9)$$

The connectivity of covalent chemical frameworks is set by the bonding arrangement of the atoms. For example, in all but the densest silicates each silicon is bonded to four oxygen atoms. Further, this situation favours tetrahedral coordination around each silicon (or framework aluminium) atom, favouring ring sizes of at least five. Thus, most silicates are hyperbolic (cf. Eq. (8)). The conventional geometric parameters of covalent frameworks – preferred bond lengths, bond angles and torsion – can be translated to give a preferred Gaussian curvature for the framework, which, by the argument above, is necessarily negative (HYDE, 1993a; HYDE *et al.,* 1993). The standard concepts of solid-state chemistry then imply a preferred Gaussian curvature for silicate networks – i.e. a homogeneous hyperbolic surface on which the silica lies. The formation of networks lying on crystalline hyperbolic surfaces is, in the light of this argument, quite natural.

This thesis is a controversial one and further work is required to determine its general applicability. However, it does lead to useful insights regarding the silicate density and the link between density and ring sizes in the framework, noted elsewhere (HYDE, 1993a; HYDE *et al.,* 1993). Further, it allows for clear definition of the pore geometry in low-density silicates, such as zeolites. Many other silicates form nets on crystalline hyperbolic surfaces that self-intersect (and are not embedded), leading to three, two-, one- and zero-dimensional channel systems (FISCHER and KOCH, 1996).

The non-euclidean approach also affords particularly simple estimates of relative energies of schwarzites, graphitic tubes and fullerenes, derived from plate elasticity theory (applied to graphitic monolayers!) (HYDE and O'KEEFFE, 1996) and suggests common stability criteria for both molecular assemblies, such as liquid crystals, and atomic crystals. At a more philosophical level, this description challenges conventional notions of dimensionality in these systems.

A two-dimensional hyperbolic perspective also offers novel insights into structures and genesis of so-called "bicontinuous phases" (such as cubic phases) in surfactant-water systems. Here too, the complex convoluted forms adopted by these systems can be traced to the requirement of a homogeneous hyperbolic structure, a frustration best relieved by the formation of IPMS or similar structures.

These structures are not bonded by the strongly directional covalent linkages present in the atomic frameworks considered above. Rather they are held together by hydrophobic and other weak interactions. A topological analysis based on ring sizes is thus not useful in these molecular systems. Another feature of hyperbolic geometry is at work in these systems. The lipid layers are themselves made up of chemically distinct components: their head-groups are exposed to water on both external surfaces, and their interior contains the oil-like chains. So in contrast to the surface model for atomic frameworks, lipid layers are modelled by films, of finite thickness, wrapped onto surfaces. The film shape is governed by the variation of cross-sectional areas through the molecular film.

This feature can be simply demonstrated with the aid of a slice of bread and a griller. The uncooked slice can be considered a flat film. If the bread is grilled from one side only, it will emerge from the grill curved exclusively towards the cooked face – the once-flat slice is now elliptic. This curvature is due to the fact that the heated bread surface has shrunk in area compared with the other, cooler, surface. Now grill the bread on the other side. The resulting toast is no longer elliptic, but hyperbolic, resembling a saddle. In this case, *both* external faces have shrunk compared to interior – a situation that can only be resolved by the formation of a saddle (Fig. 27).

If a potato slice is substituted for the bread, deep-frying the potato forms a potato crisp. Here too, surface shrinkage results in the characteristic saddle-shaped potato crisp, shown in Fig. 16. (The blistered, elliptic crisps in Fig. 17 are presumably due to local moisture gradients that result in some stretching of the surface.)

A lovely example of our poor intuition of hyperbolic forms is displayed in Fig. 28, which reveals a most unlikely form for a potato crisp: the crisp is elliptic, its boundary hyperbolic! The image is reminiscent of Cramptons' euclidean boxes; here the hyperbolic form is recognisably curved, yet its form has been "shoehorned" into a more familiar elliptic geometry.

A similar explanation accounts for the shape of tenside assemblies in water. The form of these assemblies depends on many factors; the most important being

Figure 28. Roman signwriter's view of an unlikely elliptic potato crisp, whose boundary is hyperbolic (cf. Fig. 16).

molecular shape and water content. The molecular shape can be characterised by a generalised shape parameter, related to the difference in cross-sectional area at both ends of the molecule. If these areas are equal, aggregation of the molecules into a sheet can be accommodated without any curving of the sheet. If the head-group cross-sectional area is less than that at the chain ends, the sheet must curve towards the head-groups to accommodate the cone-shaped molecules, just as the slice of bread toasted on one side only curves elliptically (Fig. 29). The form of the molecular monolayer is thus dictated by the area difference across the monolayer (ISRAELACHVILI *et al.,* 1976; HYDE, 1990). If the molecules assemble to form a bilayer, three surface areas must now be accommodated – the two head-group areas on both external faces of the bilayer, and the area of the mid-surface through the bilayer, set by the chain-ends (Fig. 30).

Again, if all of these areas are equal, the bilayer is flat. If the head-group area exceeds the that of the chain ends, the configuration is frustrated in euclidean three-space, and a "blistered" bilayer results (cf. the bubbles in crisps). If the cross-sectional area of the mid-surface set by the chain-ends is larger than that of the outer faces (set by the head-group area), the bilayer must warp – just as the toast cooked on both sides – and adopt a hyperbolic geometry. These average molecular dimensions determine a preferred Gaussian curvature of the bilayer. If the bilayer contains a single chemical species, that preferred curvature has a single value, and the resulting membrane morphology is one that satisfies that value as nearly as possible within the constraints of
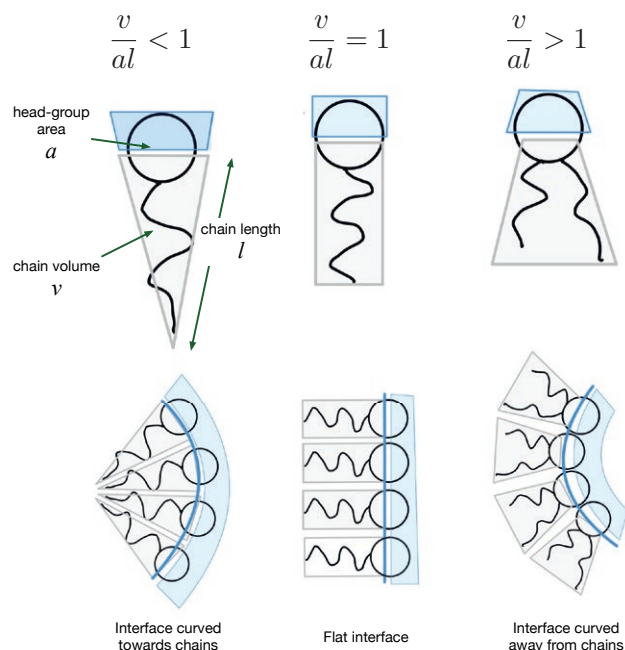
$$\frac{v}{al} < 1 \qquad \frac{v}{al} = 1 \qquad \frac{v}{al} > 1$$

head-group area *a*

chain length *l*

chain volume *v*

Interface curved towards chains

Flat interface

Interface curved away from chains

Figure 29. Schematic view of the relation between the average "wedge-shape" of a lipid or surfactant molecule (top) and the curvature of a monolayer of such molecules immersed in water (bottom).

Figure 30. Left: View of a hyperbolic molecular bilayer, showing the (green) interface, which traces the surface running through the centre of the bilayer between the chain ends and parallel interfaces (blue) traced out by the head-groups in both monolayers. Right: Global view of one possible hyperbolic bilayer geometry – the P-surface.

three-dimensional euclidean space. Clearly then homogeneous geometries are preferred, and the formation of (meso)crystalline hyperbolic membranes – as in cubic phases – is not surprising (Fig. 30).

The formation of curved films due to area mismatch between parallel layers is also common in atomic systems. A beautiful example of this is the mineral imogolite, found around the base of tropical volcanoes. Imogolite consists of two bonded layers: silica and gibbsite (CRADWICK *et al.,* 1972) (Fig. 31). The slight differences in bonding dimensions between these two structures lead to a mismatch of areas, which is accommodated by regular curving of the alumino-silicate sheets, into long 20 Å cylinders (HYDE, 1993b). The formation of cylinders, of zero Gaussian curvature, is possible without changing the local atomic arrangement (i.e. ring sizes, connectivity) in either (originally) layer, viz. regular hexagonal nets. That follows from Eqs. (6) and (7), since the integral curvature remains zero, and so the effective Euler characteristic also remains zero. Hyperbolic and elliptic forms – structured at larger distances than are usually associated with atomic structures – are also likely in other silica composites, such as allophane, asbestos, and many serpentines.

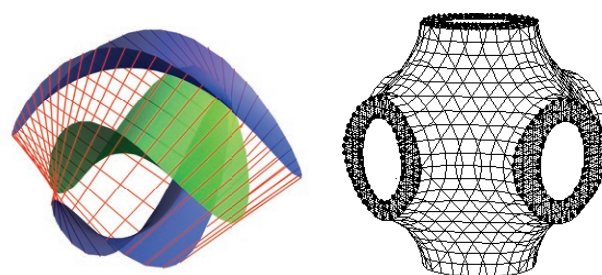Solids can also be structured at the ultrastructural level – typically microns. The biological world is replete with examples of such materials, particularly in animal skeletons. A striking example can be found in the hard calcite plates in many sea-urchins. Scanning EM images reveal complex "fenestrated" crystals, whose morphology bears remarkable resemblance to the P-surface (NISSEN, 1969; DONNAY and PAWSON, 1969). There is some distortion of the cubic symmetry of the *P* morphology, perhaps enough to reflect the underlying rhombohedral symmetry of calcite (Fig. 32). Here the calcite gives the sea-urchin a lightweight suit of armour: it is riddled with tunnels, and its strength-to-weight ratio exceeds that of concrete!

One side of the surface contains the hard inorganic calcite crystal, the other the life-giving proteins. How does this extraordinary ultrastructure form? Clearly, it is influenced by the presence of proteins, both water-insoluble structural ones and soluble material. Could it be that the proteins assemble to form an ultrastructured aqueous container – in the shape of one labyrinth system of the P-surface – in which the calcite is precipitated? It is likely to be more complex than pure templating. For example, smoothly curved magnesian calcites can be crystallised *in vitro* from solutions containing small amounts of organic additives, such as citric acid (F. C. Meldrum, private communication) suggesting that occluded proteins within the crystal assist in the formation of the curved surfaces.

Perhaps the most enigmatic feature of these shells is their glassy properties, conchoidal fracture and smoothly curved faces – coupled with apparently perfect crystallinity (as evidenced by X-ray diffraction) (LOWENSTAM and WEINER, 1989). Note, however, that the fractures along individual traberculae are often flat, and typical of cleavage planes of calcite.

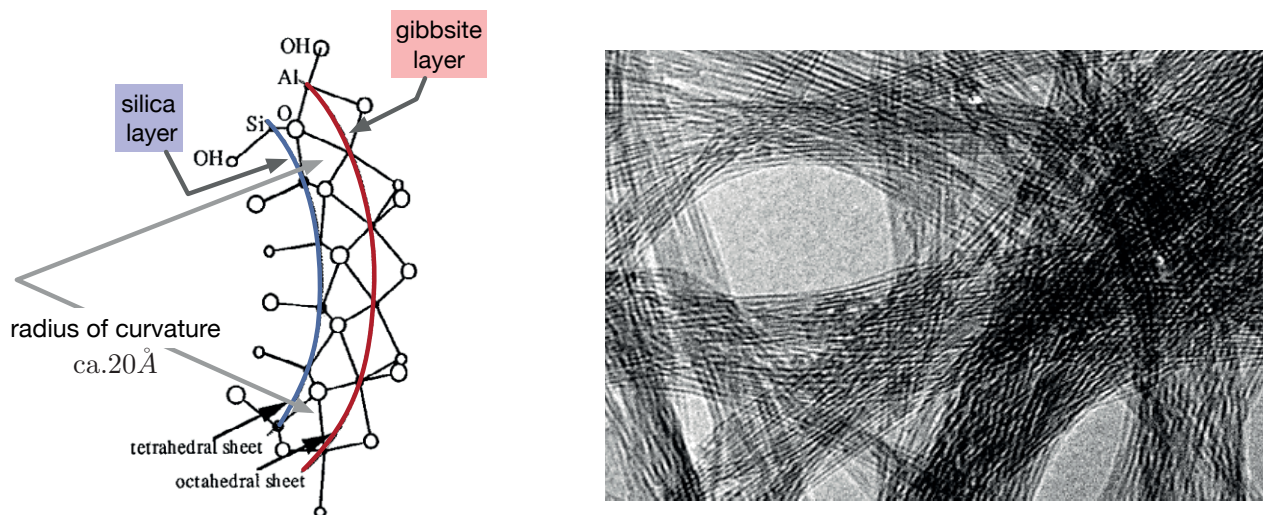It may be more than coincidental that smoothly curved inorganic crystal aggregates (alkiline earth car-

Figure 31. (Left) Cross-section through a sector of cylindrical imogolite sheet (image adapted from CRADWICK *et al.,* 1972) (Right) Electron microscopic image of imogolite cylinders (scale bar 200 Å, image adapted from WADA, 1987).
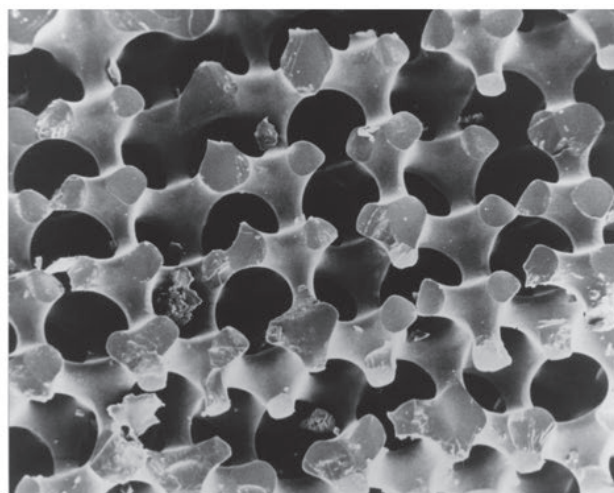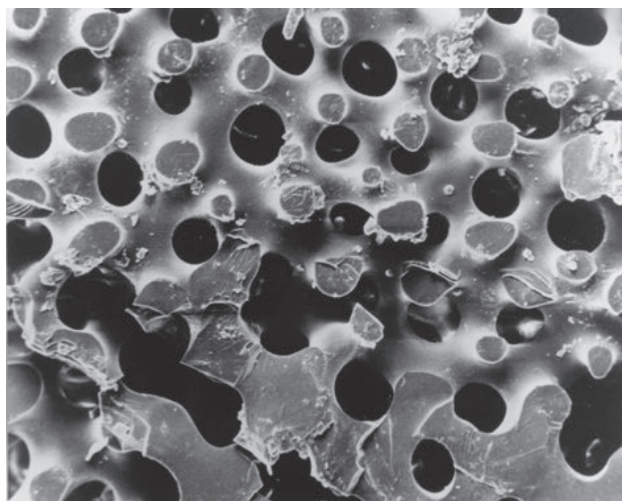

Figure 32. Scanning EM images of a skeletal plate of the sea-urchin Cidaris rugosa, after chemical treatment of the plate to remove proteinaceous tissue which lines the open channels in the living creature. The channels are microns wide (images courtesy Hans-Udde Nissen).

bonates, including calcite) can be "crystallised" in silica gels to form smoothly curved shapes, that act optically as single crystals, but whose diffractions patterns are powder-like (GARCIA-RUIZ, 1985; GARCIA-RUIZ and MORENO, 1997). The formation of curved morphologies is conventionally ascribed to the biological realm, yet these aggregates are purely inorganic (Fig. 33).

A final example is the mineral, saddle dolomite, which exhibits well-defined crystallinity, yet grows to form smoothly curved faces, with radii of curvature of the order of centimetres. The origins of curvature in this mineral (and related minerals such as ankerite) are

unclear: its very occurrence severely strains conventional three-dimensional euclidean pictures of crystals and crystal growth.

6. FINAL THOUGHTS

This exploration of the world of condensed matter has been designed to highlight the often forgotten active role of space and geometry in our perceptions of form and shape. Indeed, it has been argued by a number of respectable scientists that much of physics is no
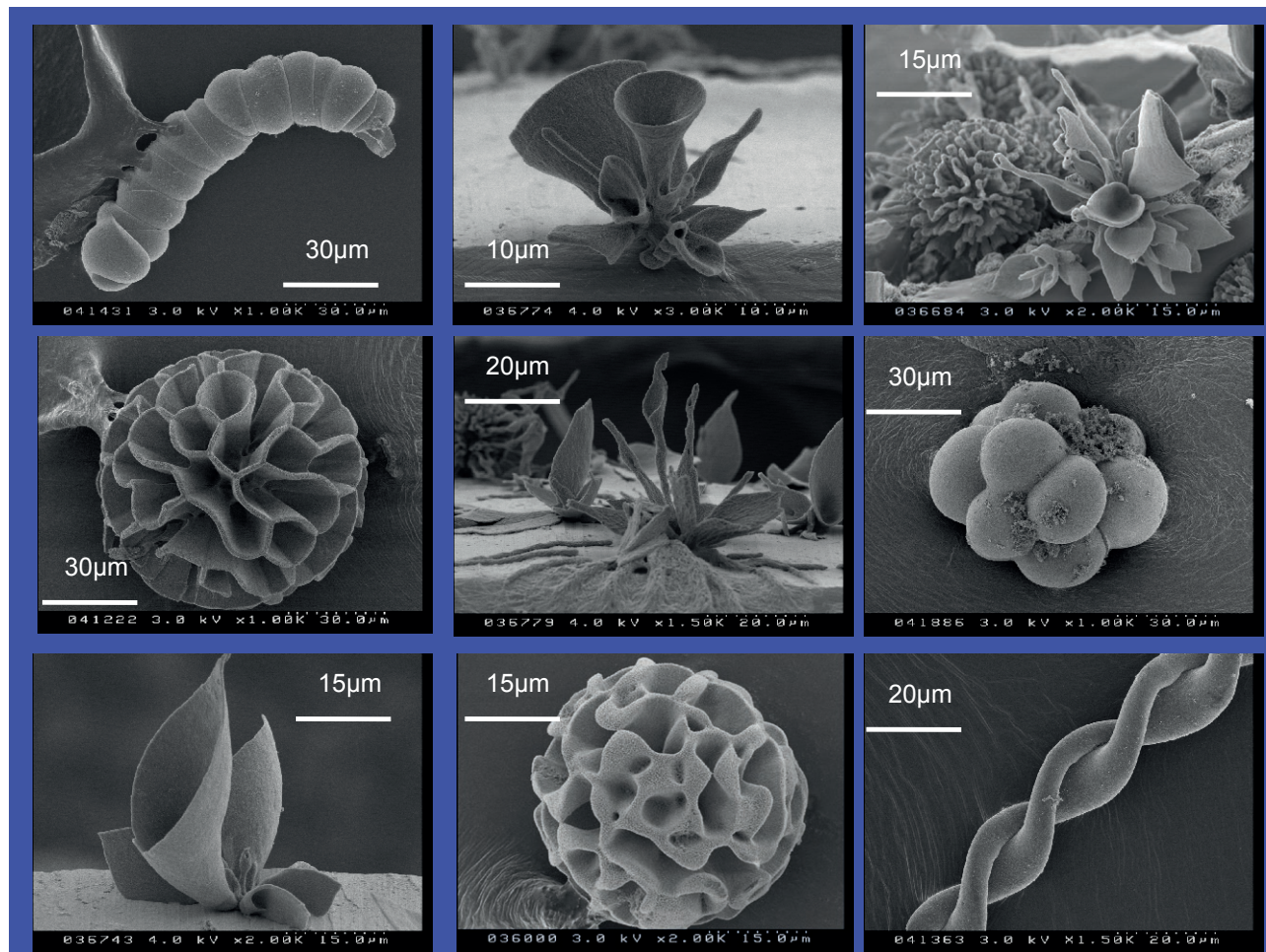
Figure 33. Field emission scanning EM images of barite crystals grown in silica gels (pH ca. 12, photo courtesy Anna Carnerup).

more than geometry; witness the remarkable statement of Arthur Stanley Eddington, the noted British cosmologist, earlier this century: "A *field of force represents the discrepancy between the natural geometry of a coordinate system and the abstract geometry arbitrarily assigned to it*". This idea, only possible post Riemann, bears some reflection. At the smallest length scale, in the sub-atomic world and at huge length scales, in the cosmological Universe, the assumed geometry of a reference frame is laid bare, and scientists regularly confront issues of dimensionality and curvature. Yet those of us probing matter between these extremes of length persist with the familiar euclidean assumptions. In 1959, Lancelot Whyte wrote, *"Exact science is mainly built on the sense of sight, and if no one has ever seen a straight line 'looking straight', or rather if no one knows exactly what that means, and if continuous straight objects are really open patterns of discrete particles, why does physical theory still prefer to assume that the fundamental laws are engraved on continuous rectangular frames as fields extending to infinity?"*

How much does Whyte's complaint hold true for biology and chemistry? Let's go back to the Tahitian islands, and the humble *Partula* of Crampton. Recall his nearly one million measurements of the form of the *Partula* shell, and detailed statistical analyses? Following our exploration of elliptic and hyperbolic forms, it seems desperately crude to engrave the exquisite swirls and twists of these shells on Crampton's rectangular frame! Rather, curvature and torsion seem to be the outstanding morphological features of these shells. How that curvature and torsion is encoded during growth of the shells is unknown, but – given the extraordinary ability of organic "soft matter" such as lipids and proteins to fashion the morphology of "hard" inorganic matter – the general features of the form itself should not surprise us. That form is far removed from Crampton's carefully drawn rectangles, boxing *Partula* forever in a euclidean grid.

REFERENCES

ALFREDSSON, V. and M. W. ANDERSON (1996) Structure of MCM-48 revealed by transmission electron microscopy, *Chem. Mater.,* **8,** 1141-1146.

BECK, J., J. VARTULI *et al.* (1992) A new family of mesoporous molecular sieves prepared with liquid crystal templates, *J. Am. Chem. Soc.,* **114,** 10835.

BLUM, Z., S. T. HYDE and B. W. NINHAM (1993) Adsorption in zeolites, dispersion self-energy and Gaussian curvature, *J. Phys. Chem.,* **97,** 661-665.

CORKERY, R. (1998) Artificial biomineralisation and metallic soaps, Ph.D. Thesis, Australian National University, Canberra.

CRADWICK, P. D. G., V. C. FARMER, J. D. RUSSELL, C. R. MASSON, K. WADA and N. YOSHINAGA (1972) Imogolite, a hydrated aluminium silicate of tubular structure, *Nature Physical Science,* **240,** 187-189.

DONNAY, G. and D. L. PAWSON (1969) X-ray diffraction studies of echinoderm plates, *Science,* **166,** 1147. FISCHER, W. and E. KOCH (1996) Spanning minimal surfaces, *Phil. Trans. Roy. Soc. Lond. A,* **354,** 2105-2142. GARCIA-RUIZ, J.-M. and A. MORENO (1997) Growth behaviour of twisted ribbons of barium carbonate/silica self-assembled ceramics, *An. Quimica Int. Ed.,* **93,** 1-2.

GOULD, S. J. (1993) *Eight Little Piggies,* Jonathon Cape, London.

GUNNING, E. S. (1965) The greening process of plastids in plants, *Protoplasma,* **60,** 111.

HAJDUK, D. A., P. E. HARPER, S. M. GRUNER, C. C. HONEKER, G. KIM, E. L. THOMAS and L. J. FETTERS (1994) The gyroid. A new morphology in weakly segregated diblock copolymers, *Macromolecules,* **27,** 4063.

HASEGAWA, H., H. TANAKA, K. YAMASAKI and T. HASHIMOTO (1987) Bicontinuous microdomain morphology of block copolymers. 1. Tetrapod-network structure of polystyrene-polyisoprene diblock polymers, *Macromolecules,* **20,** 1651-1662.

HASEGAWA, H., Y. NISHIKAWA, S. KOIZUMI, T. HASHIMOTO and S. HYDE (1993) Some new aspects on the microdomain structures in block copolymer systems, *3rd IUMRS International Conference on Advanced Materials* (IUMRS-ICAM-93), Elsevier & MRS, Japan.

HYDE, S., B. NINHAM, S. ANDERSSON, Z. BLUM, T. LANDH, K. LARSSON and S. LIDIN (1997) *The Language of Shape,* Elsevier, Amsterdam.

HYDE, S. T. (1990) Curvature and the global structure of interfaces in surfactant-water systems, *J. Physique (Coll.),* **C-7,** 209-228.

HYDE, S. T. (1993a) Crystalline frameworks as hyperbolic films, in *Defects and Processes in the Solid State. Some Examples in Earth Sciences,* edited by J. D. FitzGerald and J. N. Boland, Elsevier, Amsterdam. HYDE, S. T. (1993b) The density of three-dimensional nets, *Acta Cryst.,* A50, 753-759.

HYDE, S. T. (1993) Hyperbolic and elliptic layer warping in some sheet alumino-silicates, *Phys. Chem. Minerals,* **20,** 190-200.

HYDE, S. T. and M. O'KEEFFE (1996) Elastic warping of graphitic carbon sheets: relative energies of some fullerrenes, schwarzites and buckytubes, *Phil. Trans. Roy. Soc. Land.* A, **354,** 1999-2008.

HYDE, S. T., Z. BLUM and B. W. NINHAM (1993) The density of silicon-rich zeolite frameworks, *Acta Cryst.,* **A49,** 586-589.

ISRAELACHVILI, J. N., D. J. MITCHELL and B. W. NINHAM (1976) Theory of self-assembly of hydrocarbon amphiphiles into micelles and bilayers, *J. Chem. Soc. Faraday Trans. 2,* **72,** 1525-1568.

KROTO, H. and K. MACKAY (1988) The formation of quasi-icosahedral spiral sheet carbon particles, *Nature,* **331,** 328-331.

LANDH, T. (1995) From entangled membranes to eclectic morphologies – cubic membranes as sub-cellular space organizers, *FEBS Lett.,* **369(1),** 13-17.

LENOSKY, T., X. GONZE, M. TETER and V. ELSER (1992) Energetics of negatively curved graphitic carbon, *Nature,* **355,** 333-335.

LOWENSTAM, H. and'S. WEINER (1989) *On Biomineralization,* Oxford University Press, Oxford. LUZZATI, V. and P. A. SPEGT (1967) Polymorphism of lipids, *Nature,* **215,** 701-704.

MACKAY, A. L. and H. TERRONES (1991) Diamond from graphite, *Nature,* **352,** 762.

MEIER, W. M. and D. H. OLSON (1992) *Atlas of Zeolite Structure Types,* Butterworth-Heinemann, London.

NISSEN, H.-U. (1969) Crystal orientation and plate structure in echinoid units, *Science,* 166, 1150-1152.

O'KEEFFE, M. and B. G. HYDE (1996) *Crystal Structures. 1. Patterns and Symmetry,* American Mineralogical Society Monograph, Washington, D.C.

O'KEEFFE, M., G. B. ADAMS and 0. F. SANKEY (1992) Predicted new low energy forms of carbon, *Phys. Rev. Lett.,* **68**(15), 2325-2328.

SCHOEN, A. H. (1970) Infinite periodic minimal surfaces without self-intersections, N.A.S.A. Technical Report #D5541.

STILLWELL, J. (1982) Translation of Beltrami's essay on the interpretation of non-euclidean geometry, Mathematics Dept., Monash University, Melbourne, Australia.

TERRONES, H. and A. L. MACKAY (1992) The geometry of hypothetical curved graphite structures, *Carbon,* **30**(8), 1251-1260.

THURSTON, W. (1997) *Three-Dimensional Geometry and Topology,* Princeton University Press, Princeton.

VON SCHNERING, H.-G. and R. NESPER (1987) How nature adapts chemical structures to curved surfaces, *Angew. Chem. Int. Ed. Engl.,* **26**, 1059-1080.